SIX DAYS ■ THREE CONFERENCES ■ ONE EXHIBITION

EUROPEAN MICROWAVE WEEK 2019
PARIS EXPO PORTE DE VERSAILLES, PARIS, FRANCE
1 place de la Porte de Versailles
29TH SEPTEMBER - 4TH OCTOBER 2019

EuMW 2019
UNIVERSALITY THROUGH MICROWAVES
EUROPEAN MICROWAVE WEEK
PORTE DE VERSAILLES
PARIS, FRANCE
29TH SEPT - 4TH OCT 2019
www.eumweek.com

EUROPEAN MICROWAVE WEEK 2019

CONFERENCE PROGRAMME

EUROPE'S PREMIER MICROWAVE, RF, WIRELESS AND RADAR EVENT

Register online at:

www.eumweek.com

EuMA
European Microwave Association

Official Publication: Microwave Journal

Organised by: horizon house

Supported by: IET The Institution of Engineering and Technology

Co-sponsored by: MTT-S

Co-sponsored by: IEEE

EuMIC 2019
The 14th European Microwave Integrated Circuits Conference
Co-sponsored by:

49TH EUROPEAN MICROWAVE CONFERENCE 2019
The 49th European Microwave Conference
Co-sponsored by: EurAAP

EuRAD 2019
The 16th European Radar Conference
Co-sponsored by: EurAAP AESS

E05	E08
EuMC01 **Passive Devices - Theory and Applications** Chair: Florence Podevin[1] Co-Chair: Anthony Ghiotto[2] [1]RFIC Lab, [2]Bordeaux INP, IMS Laboratory	**EuMC02** **High Directivity Antennas** Chair: Diego Masotti[1] Co-Chair: Martino Aldrigo[2] [1]University of Bologna, [2]IMT

08:30 - 08:50

EuMC01-1
Passive Ferrite Devices: Original Designs and New Challenges for the Future's Applications
Hamza Turki[1]
[1]INOVEOS SAS

EuMC02-1
From Antenna Measurement to 5G OTA – a Paradigm Shift
Benoit Derat[1]
[1]Rohde & Schwarz GmbH & Co. KG

08:50 - 09:10

EuMC01-2
Self-Heating Study on a First Order Filter with Discrete and Continuous Tuning
Miguel Sanchez-Soriano[1], Rozenn Allanic[2], Vincent Le Saux[3], Hassan Bouazzaoui[4], Alexandre Manchec[4], Cédric Quendo[2]
[1]University of Alicante, [2]Lab-STICC-Université de Bretagne Occidentale, [3]ENSTA-Bretagne, [4]Elliptika [GTID]

EuMC02-2
Analysis and Design of Arrays with Tilted Directive Dipole Elements
Cristina Yepes[1,2], Erio Gandini[2], Stefania Monni[2], Frank E. van Vliet[2], Andrea Neto[1], Daniele Cavallo[1]
[1]Delft University of Technology, [2]TNO Defense, Safety and Security

09:10 - 09:30

EuMC01-3
Broadband Phase Control in Frequency and Time Domains: Design of True Delay-Lines for Noise-Decorrelation in Sensor-Arrays
Sidina Wane[1], Damienne Bajon[2]
[1]eV-Technologies, [2]ISAE SUPAERO Université de Toulouse

EuMC02-3
Dual-polarized Leaky Wave Antenna with Low Cross-polarization Based on the Mode Composite Ridged Waveguide
Yihong Su[1], Xian Qi Lin[1], Yong Fan[1], Yunlong Lu[2], Gaoming Xu[2]
[1]University of Electronic Science and Technology of China, [2]Ningbo University

09:30 - 09:50

EuMC01-4
Modal Analysis and Same-Bandedge Response Optimization of 3-D Lumped Networks
Yelei Yao[1,2], Mustafa S. Bakr[1], Ian Hunter[1]
[1]University of Leeds, Leeds, United Kingdom, [2]University of Electronic Science and Technology of China

EuMC02-4
Substrate-Superstrate Leaky-Wave Antenna with Interleaved Metasurfaces for Directivity Improvement
Silvia Tofani[1], Walter Fuscaldo[1], Paolo Burghignoli[1], Paolo Baccarelli[2], Alessandro Galli[1]
[1]Sapienza University, [2]Roma Tre University

09:50 - 10:10

EuMC01-5
Arbitrary Terminated Negative Group Delay Circuit with Constant Signal Attenuation and Its Application to Absorptive Bandstop Filter
Girdhari Chaudhary[1], Wang Qi[1], Jongsik Lim[2], Yongchae Jeong[1]
[1]Chonbuk National University, [2]Soonchunhyang University

EuMC02-5
A High Directivity Beam-Steering Parasitic Antenna Array
Husnain Ali Kayani[1], Christophe Craeye[1]
[1]Université catholique de Louvain

Arbitrary Terminated Negative Group Delay Circuit with Constant Signal Attenuation and Its Application to Absorptive Bandstop Filter

Girdhari Chaudhary[#1], Wang Qi[#], Jongsik Lim[*], Yongchae Jeong[#2]
[#]Division of Electronics and Information Engineering, Chonbuk National University, Republic of Korea
[*]Department of Electrical and Communication Engineering, Soonchunhyang University, Republic of Korea
[1]girdharic@jbnu.ac.kr, [2]ycjeong@jbnu.ac.kr

***Abstract* — This paper presents a design of transmission-type arbitrary terminated negative group delay (NGD) circuit with constant signal attenuation (SA). In the proposed circuit, the specified NGD and SA response can be designed by handling the characteristic impedance of transmission lines. Analytical analysis disseminates that the input and output ports of the proposed NGD circuit can perfectly match at a center frequency (f_0) without extra matching networks. The proposed analytical equations can also apply to design an arbitrary terminated absorptive bandstop filter with prescribed NGD. For an experimental confirmation, a prototype of the transmission-type NGD circuit was at the f_0 of 2.14 GHz. The experimental results are consistent with simulated and analytical results.**

***Keywords* — Abnormal group delay, constant signal attenuation, negative group delay (NGD), positive group delay (PGD), series-fed antenna arrays.**

I. INTRODUCTION

Propagation of electromagnetic waves in dispersive media can be defined by phenomena incorporating abnormal phase, group delays (GDs), and velocities [1]. Abnormal group velocities incorporate superluminal and even negative group velocities (NGVs). The negative group delay (NGD) and NGV intimate each other and they convey that peak of a pulse envelope appears from the medium at an instant before the peak of the pulse penetrate the medium. Such an ostensibly anti-causal phenomenon does not breach the principle of causality because turn-on and -off points of the wave packet propagate with a positive delay in agreement with the causality requirements [2].

To recognize the reality of the NGD, the group velocity can be revealed as (1) for homogeneous media or effective homogeneous periodic structures described by a propagation constant (β) and refractive index n [1].

$$v_g = \frac{\partial \omega}{\partial \beta} = \frac{c}{n + \omega \dfrac{\partial n}{\partial \omega}}, \tag{1}$$

where c and ω are the speed of light in vacuum and angular frequency, respectively. From (1), it is evident that if n decreases rapidly with respect to ω, the group velocity and the GD can become negative. In short, NGV or NGD exists near an absorption line or signal attenuation (SA) condition, where "anomalous" wave propagation effects can occur [1]-[3].

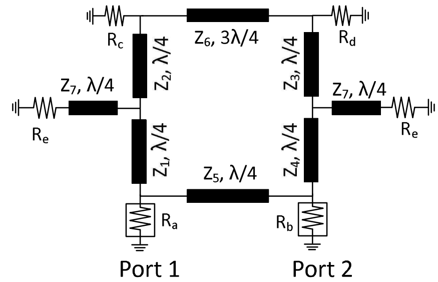

Fig. 1. Proposed structure of transmission-type arbitrary terminated NGD circuit with constant signal attenuation

The NGD circuits have been practically implemented in communication systems for lessening delay lines, improving the efficiency of feedforward linear amplifiers, developing broadband constant phase shifters, achieving non-Foster reactive elements, and eliminating beam-squint in series-fed antenna arrays [3]-[7].

Series or shunt *RLC* resonators are widely used to generate the NGD at microwave frequency which can be broadly categorized into reflection- and transmission-types [8]-[10]. The reflection-type NGD circuits provide excellent input and output matchings due to inherent 90° 3-dB hybrid [8], [9], however, the transmission-type NGD circuits suffered from poor input and output matchings [10]. To improve input and output matchings in transmission-type NGD circuits, extra matching networks are required which can decrease the overall NGD [10]. In addition, the conventional NGD circuits also suffer from high SA which increases in proportional to NGD.

In recent years, reflective bandstop filters with NGD were investigated in [11], which requires additional impedance transformers for matching port impedances. In [12], an absorptive bandstop filter is designed by using resistor-loaded coupled-line structures. From the literature reviews, it is also confirmed that the conventional NGD circuits and absorptive bandstop filters have been designed only for equal termination port impedances.

In this paper, an arbitrarily terminated transmission-type NGD circuit with constant SA is explored. The proposed transmission-type NGD circuit contributes perfect input and output matchings at the center frequency (f_0) without any extra

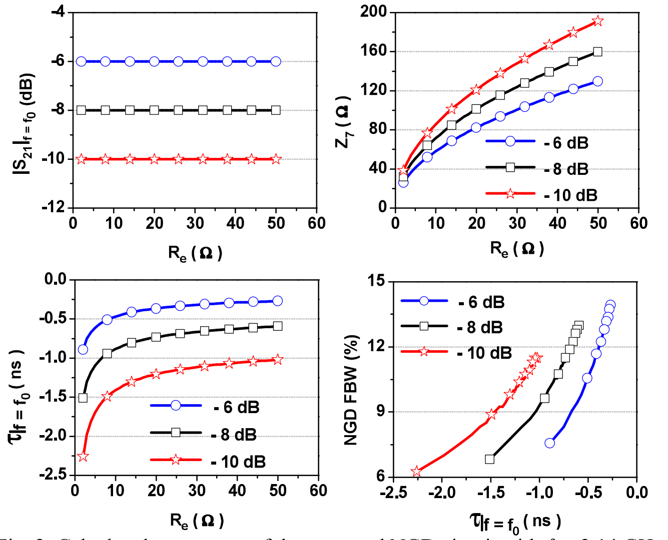

Fig. 2. Calculated parameters of the proposed NGD circuit with f_0 = 2.14 GHz, $R_a = R_b = R_c = R_d$ = 50 Ω, Z_2 = 130 Ω, n = 1 and different R_e.

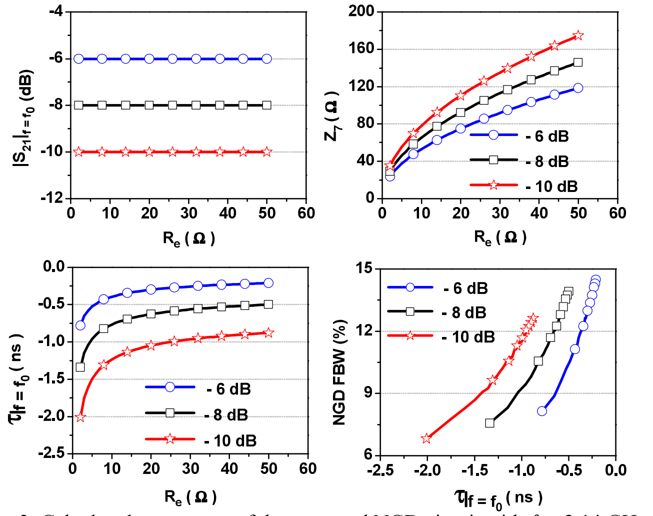

Fig. 3. Calculated parameters of the proposed NGD circuit with f_0 = 2.14 GHz, R_a = 40 Ω, R_b = 60 Ω, $R_c = R_d$ = 60 Ω, Z_2 = 130 Ω, n = 1 and different R_e.

matching networks. Analytical design equations have been supplied to calculate circuit parameters, which have been verified with simulation and experimental results. In addition, the design equations are also applicable to design the arbitrary terminated absorptive bandstop filter with the prescribed NGD.

II. Analytical Design Equations

Fig. 1 depicts the proposed structure of transmission-type NGD with arbitrarily terminated port impedances R_a and R_b. The proposed NGD circuit comprises five $\lambda/4$ transmission lines (TLs) with characteristic impedances of Z_1, Z_2, Z_3, Z_4, Z_5 and one $3\lambda/4$ TL with characteristics impedance of Z_6. Similarly, two $\lambda/4$ TLs with the characteristic impedance of Z_7 which are terminated with R_e. Finally, two resistors R_c and R_d are connected at end of $3\lambda/4$ TL. The S-parameters of the proposed NGD circuit can be determined by using (2).

$$S = -\sqrt{y}\left[Y+y\right]^{-1}\left[Y-y\right]\left[\sqrt{y}\right]^{-1}, \tag{2}$$

where

$$Y = \begin{bmatrix} Y_{11} & Y_{12} & Y_{13} & 0 \\ Y_{21} & Y_{22} & 0 & Y_{24} \\ Y_{13} & 0 & Y_{33} & Y_{34} \\ 0 & Y_{42} & Y_{43} & Y_{44} \end{bmatrix}, \quad y = \begin{bmatrix} 1/R_a & 0 & 0 & 0 \\ 0 & 1/R_b & 0 & 0 \\ 0 & 0 & 1/R_c & 0 \\ 0 & 0 & 0 & 1/R_d \end{bmatrix} \tag{3a}$$

$$Y_{11} = -j/Z_5 \cot\theta + \frac{1/Z_1\left(1/Z_{in} - j/Z_2 \cot\theta + j/Z_1 \tan\theta\right)}{1/Z_1 + j\left(1/Z_{in} - j/Z_2 \cot\theta\right)\tan\theta} \tag{3b}$$

$$Y_{22} = -j/Z_5 \cot\theta + \frac{1/Z_4\left(1/Z_{in} - j/Z_3 \cot\theta + j/Z_4 \tan\theta\right)}{1/Z_4 + j\left(1/Z_{in} - j/Z_3 \cot\theta\right)\tan\theta} \tag{3c}$$

$$Y_{33} = -j/Z_6 \cot 3\theta + \frac{1/Z_2\left(1/Z_{in} - j/Z_1 \cot\theta + j/Z_2 \tan\theta\right)}{1/Z_2 + j\left(1/Z_{in} - j/Z_1 \cot\theta\right)\tan\theta} \tag{3d}$$

$$Y_{44} = -j/Z_6 \cot 3\theta + \frac{1/Z_3\left(1/Z_{in} - j/Z_4 \cot\theta + j/Z_3 \tan\theta\right)}{1/Z_3 + j\left(1/Z_{in} - j/Z_4 \cot\theta\right)\tan\theta} \tag{3e}$$

$$Y_{13} = Y_{31} = \frac{1/Z_1 Z_2 \csc^2\theta}{j\left(1/Z_1 + 1/Z_2\right)\cot\theta - 1/Z_{in}} \tag{3f}$$

$$Y_{42} = Y_{24} = \frac{1/Z_3 Z_4 \csc^2\theta}{j\left(1/Z_3 + 1/Z_4\right)\cot\theta - 1/Z_{in}} \tag{3g}$$

$$Y_{12} = Y_{21} = j/Z_5 \csc\theta, \; Y_{34} = Y_{43} = j/Z_6 \csc 3\theta \tag{3h}$$

$$Z_{in} = Z_7 \frac{R_e + jZ_7 \tan\theta}{Z_7 + jR_e \tan\theta}, \; \theta = \pi f / 2 f_0 \tag{3i}$$

and f and f_0 are operating and design center frequency, respectively. For zero reflections ($S_{11} = S_{22} = 0$) from ports 1 and 2 at $f = f_0$, the characteristics impedances of TLs are found as (4) using (2)-(3).

$$Z_1 = \sqrt{R_a/R_c}\,Z_2 \;,\; Z_3 = \sqrt{R_d/R_c}\,Z_2 \tag{4a}$$

$$Z_4 = \sqrt{R_b/R_c}\,Z_2 \,,\, Z_5 = \sqrt{R_a R_b} \tag{4b}$$

$$Z_6 = \sqrt{R_c R_d} \tag{4c}$$

Furthermore, the magnitude of transmission coefficient at f_0 can be simplified as (5).

$$\left|S_{21}\right|_{f=f_0} = \left|S_{12}\right|_{f=f_0} = \frac{Z_2^2}{R_c Z_7^2/R_e + Z_2^2} \tag{5}$$

As can be seen from (5), the magnitude of transmission coefficient is independent on termination port impedances R_a and R_b. Using (5), the value Z_7 can be found as (6) for any specified insertion loss (α).

$$Z_7 = Z_2\sqrt{R_e/R_c\left(10^{\frac{\alpha(dB)}{20}} - 1\right)} \tag{6}$$

Finally, using the phase of S_{21}, the assessed GD can be calculated as (7) using (2)-(4).

$$\tau = \frac{1}{2\pi}\frac{d\angle S_{21}}{df} \tag{7}$$

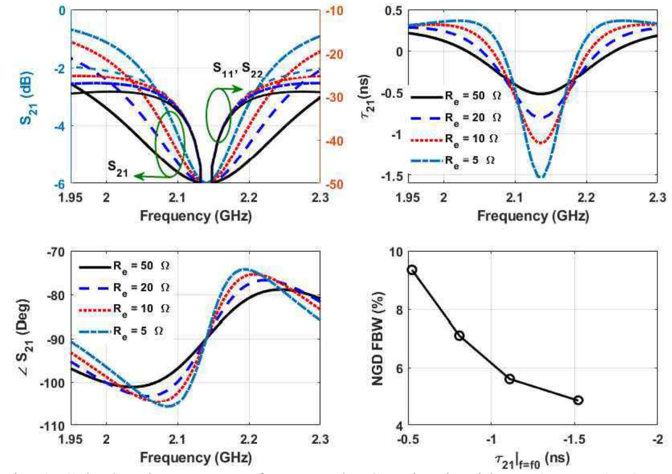

Fig. 4. Calculated responses of proposed NGD circuit with $n = 3$, $R_a = 45$ Ω, $R_b = 55$ Ω, $R_c = R_d = 50$ Ω, $Z_2 = 130$ Ω and $R_e = 5$ to 50 Ω.

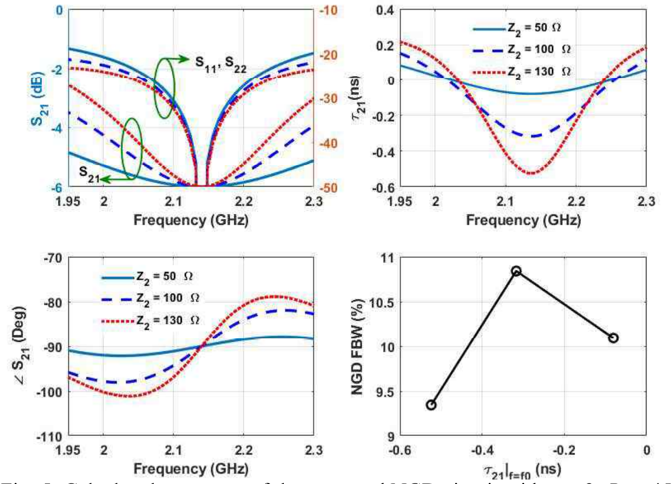

Fig. 5. Calculated responses of the proposed NGD circuit with $n = 3$, $R_a = 45$ Ω, $R_b = 55$ Ω, $R_c = R_d = 50$ Ω, $R_e = 50$ Ω and $Z_2 = 70$ to 130 Ω.

Since it is complicated to find analytical expression of GD, the MATLAB tool will be used to find value of GD numerically. Similarly, to evaluate the performance of NGD circuit, the NGD fractional bandwidth (FBW) is another relevant parameter which can be defined by (8).

$$\Delta = \frac{f_2 - f_1}{f_0} \times 100\% \quad , \tag{8}$$

where f_1 and f_2 are lower and upper cutoff frequencies in which the GD is less than zero. The values of f_1 and f_2 can be found numerical method using MATLAB for mathematically simplicity.

Based on analytical design equations, Figs. 2 and 3 illustrate the calculated parameters of the proposed NGD circuit for different constant signal attenuation. In these calculations, the value of R_e is varied from 5 to 50 Ω. The values of Z_7 and NGD FBW are increased, however, NGD value is decreased for higher value of R_e. The low value of R_e is preferable for higher NGD.

Fig. 4 shows the computed responses of the proposed NGD circuit by sweeping R_e and fixed Z_2. In this simulation, the magnitude of S_{21} at f_0 is assumed as 6 dB to illustrate the constant SA of the proposed NGD circuit. As seen from this figure, NGD can be enhanced by decreasing R_e. Similarly, Fig 5 demonstrates the responses of the proposed NGD circuit by varying Z_2 and maintaining fixed R_e. The higher NGD can be obtained if the value of Z_2 increases toward high value. However, the NGD bandwidth (bandwidth of GD < 0) of the proposed circuit is reduced if NGD is high, which necessitates a trade-off between them. As noticed from these figures, the proposed transmission-type NGD circuit provides excellent input and output return loss characteristics without any external matching networks. In addition, the phase of S_{21} is constant as GD becomes zero. This property of the proposed circuit can be applied to series-fed antenna arrays for minimizing the beam-squint problem [8].

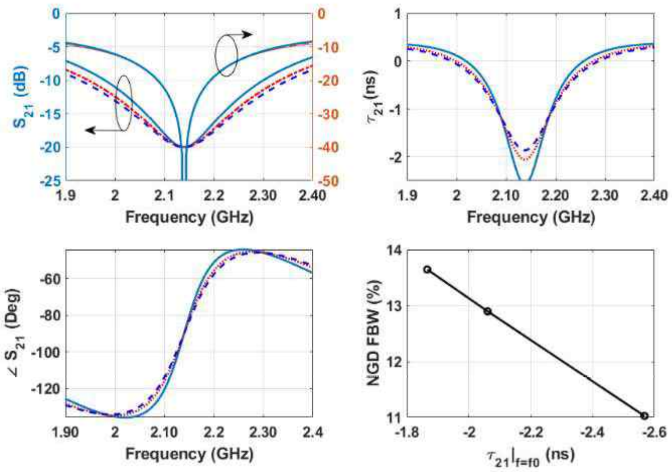

Fig. 6. Computed responses of absorptive bandstop filter with IL = 20 dB, $R_a = 55$ Ω, $R_b = 60$ Ω, $R_c = R_d = Z_2 = 50$ Ω and different R_e.

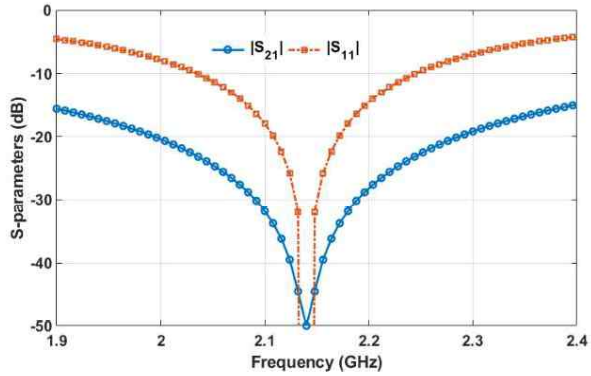

Fig. 7. Computed response of absorptive bandstop filter with IL = 50 dB, $R_a = 45$ Ω, $R_b = 55$ Ω, $R_c = R_d = 50$ Ω, $Z_2 = 50$ Ω and $R_e = 5$ Ω.

Since the SA of the proposed circuit can be specified arbitrarily, these design equations can further apply to design absorptive bandstop filter. Figs. 6 and 7 show the computed responses of the absorptive bandstop filter with the specified SA. As shown figures, the bandstop filter is perfectly matched at f_0. From these results, it can be concluded that the proposed structure can provide absorptive bandstop characteristics without additional matching circuits.

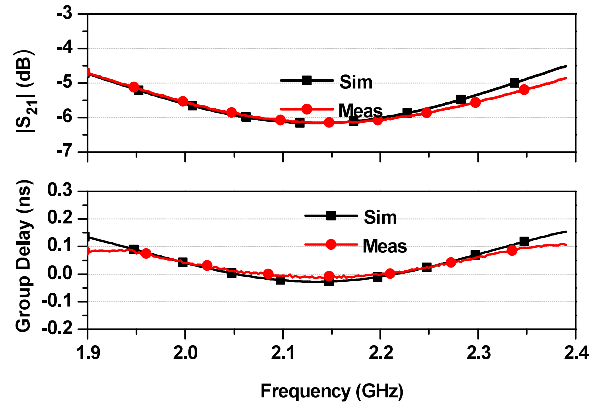

(a)

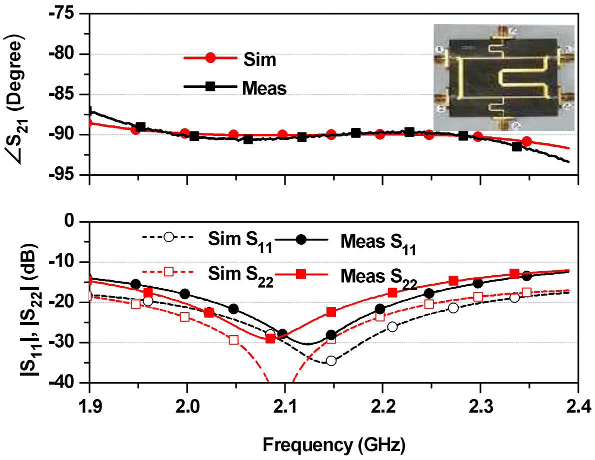

(b)

Fig. 8. Simulation and experimental results: (a) magnitude/group delay and (b) phase/return loss characteristics.

III. Experimental Results

A prototype of the proposed transmission-type NGD circuit was constructed at f_0 of 2.14 GHz for experimental validation. In this work, substrate RT/Duroid 5880 with dielectric constant (ε_r) of 2.2 and thickness (h) of 0.787 mm was used. The purpose of design example was to obtain zero GD. The termination impedances of the designed circuit are chosen as $R_a = R_b = 50$ Ω for measurement simplicity. The computed circuit parameters are summarized as $R_c = R_d = R_e = 50$ Ω, $Z_1 = Z_2 = Z_3 = Z_4 = 70$ Ω, $Z_5 = Z_6 = 50$ Ω, and $Z_7 = 69.83$ Ω.

Fig. 8(a) illustrated the experimental and results of the proposed NGD circuit. From measurement, the magnitudes of S_{21} and GD are confirmed as $|S_{21}| = -6.05$ dB and $\tau_{21} = -0.034$ ns at f_0 = 2.14 GHz. Fig. 8(b) illustrates the simulated and measured phase/return loss characteristics of the proposed NGD circuit. The return losses are experimentally confirmed as $|S_{11}| = -25.66$ dB and $|S_{22}| = -21.70$ dB at f_0, while higher than 15 dB return loss is noticed in the frequency range of 1.99 - 2.22 GHz. Also, the phase of S_{21} is almost constant over the FBW of 22.3%. The overall circuit size of the prototype circuit is 67.18 × 43.10 mm^2.

IV. Conclusion

In this paper, a design of transmission-type negative group delay circuit with constant signal attenuation is explored. From theoretical analysis, it is shown that the group delay can be enhanced by extending characteristic impedance and electrical lengths (odd-multiple of $\lambda/4$) of the transmission line, whereas the magnitude of transmission coefficients remains constant at a center frequency. For validation, a prototype circuit with zero group delay was demonstrated at the center frequency of 2.14 GHz. The proposed power divider can be applicable for high power amplifiers, active antenna arrays, and minimizing the beam-squint problem of phased-array antennas.

Acknowledgment

This research was supported by the Basic Science Research Program through the National Research Foundation of Korea (NRF) funded by the Ministry of Education, Science and Technology (2016R1D1A1A09918818) and in part by Korean Research Fellowship Program through the National Research Foundation of Korea (NRF) funded by Ministry of Science and ICT (2016H1D3A1938065).

References

[1] L. Brillouin, and A. Sommerfeld, *Wave Propagation and Group Velocity*, 1960, pp. 113-137.

[2] C. H. Hymel, M. H. Skolnick, R. A. Stubbers, and M. E. Brandt, "Temporally advanced signal detection: a review of technology and potential applications," *IEEE Circuit and Systems Magazine*, vol. 11, pp. 10-25, 2010.

[3] H. Choi, Y. Jeong, C. D. Kim, and J. S. Kenney, "Efficiency enhancement of feedforward amplifiers by employing a negative group delay circuit," *IEEE Trans Microwave Theory Tech*, vol. 58, no. 5, pp. 1116-125, May 2010.

[4] H. Mirzaei and G. V. Eleftheriades, "Arbitrary-angle squint-free beamforming in series-fed antenna arrays using non-Foster elements synthesized by negative group delay networks," *IEEE Trans. Antenna and Propagation*, vol. 63, no. 5, pp. 1997-2010, May 2015.

[5] H. Mirzaei and G. V. Eleftheriades, "Realizing non-Foster reactive elements using negative group delay networks," *IEEE Trans. Microwave Theory Tech.*, vol. 61, no. 12, pp. 4322-4332, Dec. 2013.

[6] S. S. Oh, and L. Shafai, "Compensated circuit with characteristic of lossless double negative materials and its application to array antennas," *IET Microwave Antenna and Propagation*, vol. 1, no. 1, pp. 29-38, 2007.

[7] S. Keser and M. Mojahedi, "Removal of beam squint in series fed array antennas using abnormal group delay phase shifters," *Antennas and Propagation Society International Symposium (APSURSI)*, pp. 1-4, 2010.

[8] S. Lucyszyn and I. D. Robertson, "Analog reflection topology building blocks for adaptive microwave signal processing applications," *IEEE Tran. Microwave Theory Tech.*, vol. 43, no. 3, pp. 601-611, Mar. 1995.

[9] G. Chaudhary and Y. Jeong, "Low signal attenuation negative group delay networks topologies using coupled lines," *IEEE Trans. Microwave Theory Tech.*, vol. 62, no. 10, pp. 2316-2324, Oct. 2014.

[10] G. Chaudhary, Y. Jeong, and J. Lim, "Microstrip line negative group delay filters for microwave circuits," *IEEE Trans. Microwave Theory Techn.*, vol. 62, no. 2, pp. 234-243, Feb. 2014.

[11] L. Qiu, L. S. Wu, W. Y. Yin, and J. F. Mao, "Absorptive bandstop filter with prescribed negative group delay and bandwidth," *IEEE Microwave Wireless Component Letters*, vol. 27, no. 7, pp. 639-641, Jul. 2017.

[12] G. Liu, J. Xu, and Z. Liu, "A narrowband absorptive bandstop filter based on resistor-loaded compact resonator," *Progress in Electromagnetic Research Symposium (PIERS)*, May 2017.